



## Investigation of Wadi Al-Shatti Iron Oxide Effects on the Gamma Ray Attenuation and Compression Strength of Hardened Concrete

\*Mohammed A. Al Madani<sup>1</sup>, Yousef A. Abdullah<sup>2</sup>, Elfitouri K. Ahmied<sup>3</sup>, Noura S. Hawashi<sup>1</sup> and Mahmoud J. Altayeb<sup>1</sup>

<sup>1</sup>Department of Materials & Corrosion Eng, Faculty of Energy & Mining Eng, Sebha University, Libya

<sup>2</sup>Department of Physics, Faculty of Science, Sebha University, Libya

<sup>3</sup>Department of Oil Eng, Faculty of Eng, Sirte University, Libya

### Keywords:

WSIO  
Gamma Ray  
LAC  
MAC  
Apparent and Calculated Density  
Compressive Strength

### ABSTRACT

A local ore material from Wadi Al-Shatti (south west of Libya) using different concentrations were investigated as a shielding material. The linear attenuation coefficients, mass attenuation coefficients and calculated density showed that the ore material used in this study may be preferred as shielding material against gamma radiation. It is clear from the results that as the sample thickness increases, the detector intensity decreases and when percentage of Wadi Al-Shatti Iron Oxide (WSIO) increases, the linear attenuation coefficient (LAC), on the other hand, the mass attenuation coefficients (MAC) decreased. Generally, the attenuation of WSIO increases as increasing the linear attenuation coefficient. This research is also concerned with studying the effect of replacing a mix sand of concrete with different weight of WSIO namely. It was expected that addition of iron oxide material with higher density higher hardness than Portland cement will increase the compressive strength. In general, the addition of low contents of WSIO to the concrete may improve the compressive strength, but still depends on the concentration of iron oxide as well as the thickness of the concrete.

## دراسة تأثير خام حديد وادي الشاطئ على توهين أشعة جاما وتأثيره على الخواص الميكانيكية للخرسانة

\*محمد الكيلاني المدني<sup>1</sup> و يوسف أبو بكر عبدالله<sup>2</sup> و الفيتوري خليفة أحمد<sup>3</sup> و نورا سليمان حواشي<sup>1</sup> و محمود جمال الطيب<sup>1</sup>

<sup>1</sup> قسم هندسة المواد والتآكل، كلية هندسة الطاقة والتعدين، جامعة سبها، ليبيا

<sup>2</sup> قسم الفيزياء، كلية العلوم، جامعة سبها، ليبيا

<sup>3</sup> قسم هندسة البترول، كلية الهندسة، جامعة سرت، ليبيا

### الكلمات المفتاحية:

حديد وادي الشاطئ  
أشعة جاما  
معامل التوهين الخطي  
معامل التوهين الكتلي  
الكثافة الظاهري والمحسوبة  
مقاومة أجهاد الضغط

### الملخص

تم اختيار تركيزات مختلفة من خام أكسيد الحديد المحلي من وادي الشاطئ (جنوب غرب ليبيا) كمادة واقية من الإشعاع. أظهرت معاملات التوهين الخطي ومعاملات التوهين الكتلي والكثافة المحسوبة أن خام أكسيد الحديد المستخدم في هذه الدراسة قد تكون مفضلة كمادة واقية ضد أشعة جاما. يتضح من النتائج أنه كلما زاد سمك العينة تقل شدة الكاشف وعندما تزداد النسبة المئوية لأكسيد الحديد بوادي الشاطئ (WSIO)، فإن معامل التوهين الخطي (LAC) وكذلك معامل التوهين الكتلي (MAC) تنخفض. بشكل عام، يزداد توهين (WSIO) مع زيادة معامل التوهين الخطي، ويهتم هذا البحث أيضًا بدراسة تأثير استبدال مزيج رمل الخرسانة بوزن مختلف من (WSIO). كان من المتوقع أن تؤدي إضافة مادة أكسيد الحديد ذات الصلابة الأعلى كثافة من الأسمنت البورتلاندي إلى زيادة مقاومة الانضغاط. بشكل عام، قد تؤدي إضافة محتويات منخفضة من (WSIO) إلى الخرسانة إلى تحسين مقاومة الانضغاط، ولكنها لا تزال تعتمد على تركيز أكسيد الحديد وكذلك سمك الخرسانة.

### Introduction

Radiation is a part of our daily life, so radiation and life are inseparable. Today, with the development of nuclear technology, the use of radiation in different areas of industry, agriculture, and medicine is flourishing. Different rays, including X and gamma

radiation, are emitted as a result of nuclear reactions. These types of radiation have a high penetration capability in material, and if not attenuated using proper protection, they can bring serious harm to humans and cause irreparable environmental hazards. The design

Corresponding author:

E-mail addresses: [moh.ibrahim@sebhau.edu.ly](mailto:moh.ibrahim@sebhau.edu.ly), (Y. A. Abdullah) [You.Omar@sebhau.edu.ly](mailto:You.Omar@sebhau.edu.ly), (E. K. Ahmied) [e.ahmied@su.edu.ly](mailto:e.ahmied@su.edu.ly), (N. S.

Hawashi) [Nur.Hawashi@sebhau.edu.ly](mailto:Nur.Hawashi@sebhau.edu.ly), (M. J. Altayeb) [Mah.Atayeb@sebhau.edu.ly](mailto:Mah.Atayeb@sebhau.edu.ly)

Article History : Received 19 July 2022 - Received in revised form 17 August 2022 - Accepted 03 October 2022

and construction of radioactive radiation shielding for protecting people, equipment, and buildings from the harmful effects of radiation is one of the most important issues in nuclear science. Selecting and employing appropriate material may be helpful in reducing the radiation emitted by radioactive materials to the authorized level [1].

Concrete is a good radiation protector material because it has the characteristics necessary to weaken the gamma rays and neutrons [1]. The aggregate component of concrete plays an important role in improving concrete shielding properties and therefore has good shielding properties for the attenuation of X and  $\gamma$  rays [2], [3].

## 2 Basic Shielding Parameters

### 2.1. Linear Attenuation Coefficient (LAC)

The linear attenuation coefficient gives information about the effectiveness of a given material per unit thickness, in promoting photon interactions [4]. The large value of attenuation coefficient is more likely to the given thickness of material [4]. The magnitude of attenuation coefficient varies with thickness of material and its density, as we imply, with photon energy, while specific values of the attenuation coefficient will vary among materials for photons of specified energy [4]. The plots of attenuation coefficient versus photon energy are similar for different materials. In general, trends shows high values of attenuation coefficient at low photon energies that decreases as photon energy increases. The reason of these trends is that the linear attenuation coefficient is made up of three major components, each of which is depends upon different types of photon interaction [4]. At lower energy, a process is called photoelectric effect is the dominant interaction mode that has strong energy dependence, decreasing approximately as the inverse cube of the energy [4]. Linear attenuation coefficient ( $\mu$ )  $\text{cm}^{-1}$  is determined by using a well collimated narrow beam of photon passing through a homogeneous absorber of thickness 't', the ratio of intensity of emerging beam from the source along the incident direction, to the intensity is given by the Beer Lambert law [4].

$$\mu_L = \frac{\ln \frac{I}{I_0}}{X} \quad (1.1) [4] \quad \text{where, } I_0 \text{ is the incident photon intensity, } I \text{ is the transmitted photon intensity, and } X \text{ is the thickness of absorber.}$$

### 2.2. Mass Attenuation Coefficient (MAC)

The ratio of linear attenuation coefficient ( $\mu$ ) to the density ( $\rho$ ) is called the mass attenuation coefficient ( $\mu / \rho$ ) and has the dimension of area per unit mass ( $\text{cm}^2 / \text{gm}$ ). A narrow beam of mono-energetic photons with an incident intensity  $I_0$ , penetrating a layer of material with mass thickness t and density  $\rho$ , emerges with intensity I given by the following relation:

$$\mu_m = \frac{\ln \left( \frac{I}{I_0} \right)}{X_m} \quad (1.2) [5]$$

The thickness of the absorber can be calculated by the following formula:

$$X = \rho t \quad (1.3) [5]$$

### 2.3. Apparent Density (AD)

Density can be represented as the following:

$$\rho = \frac{M}{V} \quad (1.4) [6]$$

where,  $\rho$  is the apparent density,  $M$  is the mass and  $V$  is the volume.

### 2.4. Calculated Density (CD)

The calculated density gives better and accurate results than the apparent density, since the calculated density using the  $\gamma$ -ray and the mass attenuation coefficient [6]. The calculated density can be represented by the following relation:

$$\rho_s = \frac{\ln \left( \frac{I}{I_0} \right)}{\mu_m X} \quad (1.5) [6]$$

where,  $\rho_s$  is the calculated density,  $\ln \left( \frac{I}{I_0} \right)$  is the absorption logarithm,  $\mu_m$  is the mass attenuation coefficient, and  $X$  is the material thickness [6].

## 3. Iron Oxide (IO)

Properties of hematite iron oxide is shown in (Table 3.1).

**Table 3.1. Hematite Iron Oxides Properties [8]**

Density g/cm <sup>3</sup>	Colour	Cation	Formula	Oxide
5.26	Red	Fe <sup>3+</sup>	$\alpha$ -Fe <sub>2</sub> O <sub>3</sub>	Hematite
4.87	Reddish brown	Fe <sup>3+</sup>	$\gamma$ -Fe <sub>2</sub> O <sub>3</sub>	Maghemite

## 4. Literature Survey

*Mostofinejad et al.* (2012) [9] studied the mix design parameters that had an effect on the gamma ray attenuation coefficient and the strength of normal and heavy concretes. They showed that the barite concrete attenuation coefficient was 30% higher than the conventional concrete. Also, replacing cement with silica fume will diminish the concrete attenuation coefficient [9].

*Ouda* (2015) [10] investigated the suitability of some concrete components for producing high-performance, heavy-density concrete using different types of aggregates. The results indicated that the compressive strength of the high-performance, heavy-density concrete incorporating magnetite as a fine aggregate was significantly higher than that containing sand [10].

## 5. Constituent Materials and Experiments

### 5.1. Cement

Portland cement (Type 42.5 N) was used in the experiments it is produced in Zliten Cement Factory in Zliten/Libya with Libyan specifications (No. 340/2009), a type of cement shown in the (Figure 5.1).



**Figure 5.1** Sample of Portland Cement (Zliten Cement Factory, Libya)

(Table 5.1 and 5.2) show the chemical and physical requirements for ordinary Portland cement respectively [10].

**Table 5.1 Chemical Requirements for Ordinary Portland Cement [10].**

	Percent, Max.
Magnesium Oxide (MgO)	8.00
Sulphur Trioxide (SO <sub>3</sub> )	3.00
SulphideSulphur (S)	1.50
Loss on Ignition	5.00
Insoluble Residue	4.00
Chloride (Cl)	0.05

**Table 5.2 Physical Requirements for Ordinary Portland Cement [11].**

	Content Max.
Finebess	225 m <sup>3</sup> /kg
Soundness	8.0 %
SulphideSulphur (s)	1.5
Setting Time	
a) Initial setting time not less than	30 min.
b) Final setting time not more than	600 min.
Compressive Strength	
a) 72& 1 h not less than	16 MPa
b) 168 f2 not less than	22 MPa
c) 672 f4 not less than	33 MPa

### 5.2 Water

(Table 5.3) show the contents of mineral water used to hardened the ordinary Portland cement [712].

**Table 5.3 The Content of Mineral Water [12]**

	Content Max.
Sodium (Na)	52.200 %
Calcium (Ca)	04.008 %
Magnesium (Mg)	02.400 %

Bicarbonates	24.400 %
Chlorides (Cl)	12.270 %
Sulfur (S)	09.500 %
Total Dissolved Salts (T. D. S.)	100
pH	7.3

**5.3. Wadi Al-Shatti Iron oxide Analysis**

The WSIO ore sample contains 6l mass % Fe Oxide / Hydroxide, 3l mass % quartz, 5 mass % apatite, 1 mass % ilmenite, 1 mass % clay minerals and trace amounts of Zircon, rutilel / anatase, monazite, calcite and Ca Sulfate. By mass, the majority of Fe Oxide / Hydroxide occurs in the coarsest fraction and the least amount in the finest fraction [13].

**5.4. Steps of Wadi Al-Shatti Iron oxide Collecting and Dressing**

As shown on the Figure 6.2 a WSIO ore was collected and dressed as the following processes: (i) Collection of the iron oxide; (ii) Calibration of an electronic balance; (iii) Weighting of plastic bowl used to balance iron oxide; (iv) Weighing of iron oxide Collected sample; (v) Screening of iron oxide Collected sample using different mesh sizes; (vi) Weight of bowl Used to Balance Tailings and Concentrate Iron Oxide; (vii) Weighting of tailings (3 mm Mesh); (viii) Weight of Tailings (2 mm Mesh); (ix) Weight of Tailings (1 mm Mesh); (x) Weighting of Iron Oxide Concentration.

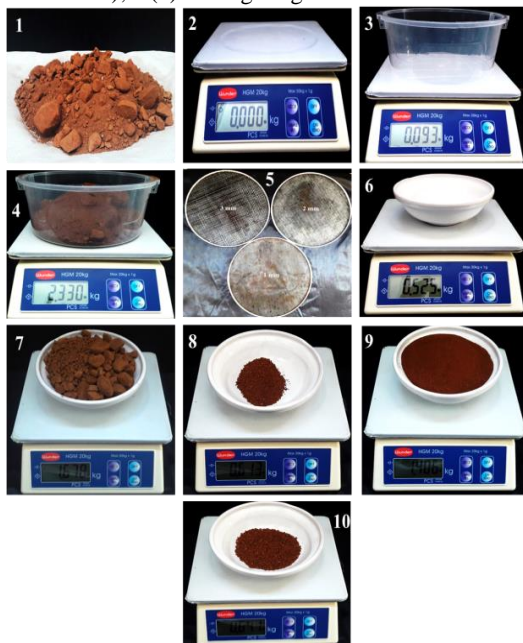


**Figure 5.2** Steps of WSIOCollecting and Dressing

**5.5 Mix Proportions**

**5.5.1. Design Requirements**

The job mix will be designed according to Standard Practice for Selecting Proportions for Normal, Heavyweight, and Mass Concrete (ACI 211.1-91). The design criteria that were used in the present research are as:

The water cement mix ratio was (0.55). The final average weight for the mix was listed in (Tables 5.5, 5.6, 5.7, and 5.8), and the applied force for a compressive test was 1560 kN.

The percentage and weight of theWSIO material and the weights of the main constituents of concrete were listed in (Tables 5.5, 5.6, 5.7, and 5.8).

**Table 5.5 Mix Design of the Concrete Samples with 0.0 % WSIOConcentration**

Sample No.	Cement (g)	Water (g)	Sand (g)	Iron Oxide(WSIO) (g)
M04	108	054	0324	000
M08	216	108	0618	000
M12	324	162	0972	000
M16	432	216	1290	000

**Table 5.6 The Mix Design of the Concrete Samples with 0.5 % WSIOConcentration**

Sample No.	Cement (g)	Water (g)	Sand (g)	Iron Oxide (WSIO) (g)
M04	108	054	320.76	03.24
M08	216	108	641.52	06.48
M12	324	162	962.28	09.72
M16	432	216	1283.04	12.96

**Table 5.7 The Mix Design of the Concrete Samples with 1.0 % WSIOConcentration**

Sample No.	Cement (g)	Water (g)	Sand (g)	Iron Oxide (WSIO) (g)
M04	108	054	0324	000
M08	216	108	0618	000
M12	324	162	0972	000
M16	432	216	1290	000

**Table 5.8 The Mix Design of the Concrete Samples with 3.0 % WSIOConcentration**

Sample No.	Cement (g)	Water (g)	Sand (g)	Iron Oxide (WSIO) (g)
M04	108	054	314.2	09.72
M08	216	108	628.56	19.44
M12	324	162	942.12	29.16
M16	432	216	1257.12	38.88

**5.6. Sample Categories**

Concrete samples were produced with and without fine powder iron oxide. In all samples, applied iron oxide was considered as a percentage of iron oxide to sand ratio (0.5%, 1.0%, and 3.0%). Obtained mixtures were molded into cylinders with diameter 6.72 cm and four different lengths of (4cm, 8cm, 12cm, and 16cm) for compression test and penetration gamma ray radiation test. The total number of plain concrete samples are 48 for ray penetration test and compression strength as showing on (Table 5.9).

**Table 5.9 Concrete Samples for Gamma Rays Penetration and Compression Test**

Iron Oxide %	Samples for ray and Compression Test				Total Samples
	4 cm	8 cm	12 cm	16 cm	
0.0	3	3	3	3	12
0.5	3	3	3	3	12
1.0	3	3	3	3	12
3.0	3	3	3	3	12

Figure (5.3) showing casted concrete samples ready for gamma ray attenuation and compression tests.



**Figure 5.3** Casted Concrete Samples Ready for Gamma Ray Attenuation and Compression Tests

**5.7 Equipment and Testing Procedure**

Cobalt 60 was used as a source of gamma ray radiation. (Figure 5.5), displays the radiation parameters of gamma ray machine. The linear attenuation coefficient, the mass attenuation coefficient, the apparent density, and the calculated density were determinedfor all concrete samples using formulas (1.1, 1.2, 1.4 and 1.5) respectively.

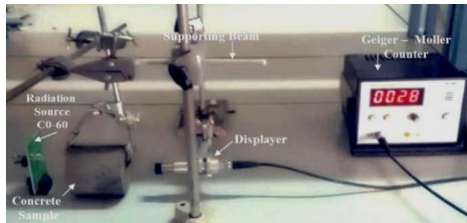


Figure 5.5 Basic Gamma Ray Source Machine

6. Experiments Results and Discussion

The penetration of  $\gamma$ -ray to concrete after 14 days from casting date using Geiger – Moller Counter to measure absorbed dose through concrete sample at different thicknesses (4cm, 8cm, 12cm, and 16cm) and different WSIO percentages (0.0 % to 3.0%).

6.1.2. Linear Attenuation Coefficient (LAC) and Mass Attenuation Coefficient (MAC)

Figures 6.1 show the exponential curves for relations between detector intensity ( $\mu\text{sv/h}$  and sample thickness cm) for concrete with several WSIO weights %. Through those figures shielding parameters such as linear attenuation coefficient (LAC) and mass attenuation coefficient (MAC) for each ratio of iron oxide was derived as shown in (Tables 6.1, 6.2, 6.3 and 6.4). It is clear from figure 6.1 that as the sample thickness increases, the detector intensity were decreased and when WSIO weight % increases, the LAC were decreased, similarly, the mass attenuation coefficients MAC were decreased as well.

Table 6.1 Concrete Samples with 0.0 % WSIO

Sample No.	X (cm)	$\mu_L$ ( $\text{cm}^{-1}$ )	$\mu_m$ ( $\text{cm}^2\text{g}^{-1}$ )	$\rho$ ( $\text{g cm}^{-3}$ )	$\rho_s$ ( $\text{g cm}^{-3}$ )
M04	04	0.3975	0.1506	2.5996	2.6002
M08	08	0.2453	0.0929	2.6033	2.5894
M12	12	0.1860	0.0688	2.6621	2.6516
M16	16	0.1464	0.0541	2.6124	2.6095

Table 6.2 Concrete Samples with 0.5 % WSIO

Sample No.	X (cm)	$\mu_L$ ( $\text{cm}^{-1}$ )	$\mu_m$ ( $\text{cm}^2\text{g}^{-1}$ )	$\rho$ ( $\text{g cm}^{-3}$ )	$\rho_s$ ( $\text{g cm}^{-3}$ )
M04	04	0.3873	0.1474	2.6276	2.6279
M08	08	0.2499	0.0951	2.6409	2.6274
M12	12	0.1860	0.0722	2.5908	2.5758
M16	16	0.1464	0.0545	2.6872	2.6869

Table 6.3 Concrete Samples with 1.0 % Iron Oxide

Sample No.	X (cm)	$\mu_L$ ( $\text{cm}^{-1}$ )	$\mu_m$ ( $\text{cm}^2\text{g}^{-1}$ )	$\rho$ ( $\text{g cm}^{-3}$ )	$\rho_s$ ( $\text{g cm}^{-3}$ )
M04	04	0.3975	0.1526	2.6042	2.6052
M08	08	0.2453	0.0946	2.6057	2.5929
M12	12	0.1860	0.0721	2.5932	2.5793
M16	16	0.1464	0.0559	2.6189	2.6187

Table 6.4 Concrete Samples with 3.0 % WSIO

Sample No.	X (cm)	$\mu_L$ ( $\text{cm}^{-1}$ )	$\mu_m$ ( $\text{cm}^2\text{g}^{-1}$ )	$\rho$ ( $\text{g cm}^{-3}$ )	$\rho_s$ ( $\text{g cm}^{-3}$ )
M04	04	0.3960	0.1523	2.5996	2.6002
M08	08	0.2493	0.0963	2.6033	2.5894
M12	12	0.1829	0.0690	2.6621	2.6516
M16	16	0.1490	0.0571	2.6124	2.6095

Table 6.5 and 6.6 show the results of LAC and MAC average for each WSIO weight % at different concrete sample thicknesses respectively. A relation has been constructed as shown on Figure 6.2, thus, it can be observed that the LAC was decreased as WSIO increased from 0.0 % to 0.5 %. The LAC was increased as WSIO increased from 0.5 % to 3.0 %. The maximum % increasing in LAC was approximately 26 % at WSIO weight 3.0 %. A relation has been constructed as shown on Figure 6.3, thus, it can be observed that the MAC was increased as WSIO increased from 0.0 % to 1.0 %. The MAC was decreased as WSIO increased from 1.0 % to 3.0 %. The maximum % increasing in MAC was approximately 2.345 % at WSIO weight 1.0 %.

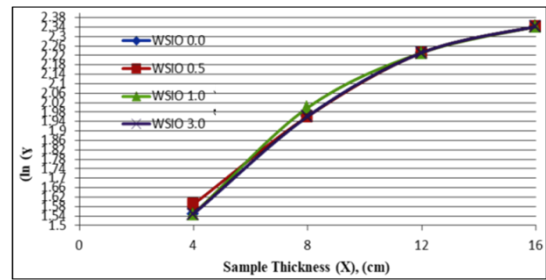


Figure 6.1 Relation of Logarithm  $\gamma$  – Ray Absorption vs. Sample Thickness with 0.0 %, 0.5 %, 1.0 %, and 0.30 % Weight of WSIO in Concrete

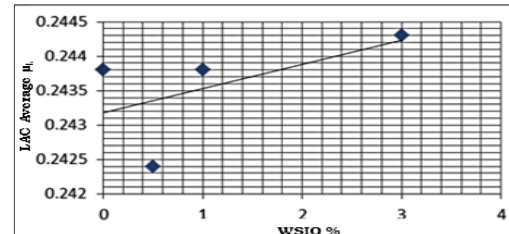


Figure 6.2 Relation of LAC Average vs. WSIO % in Concrete

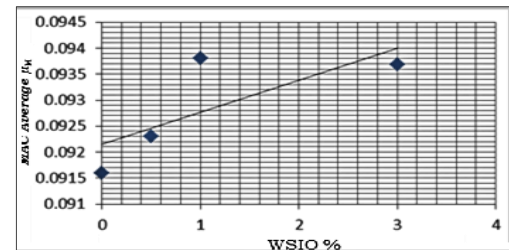


Figure 6.3 Relation of MAC Average vs. WSIO % in Concrete

Table 6.5 LAC Average Calculation

WSIO %	Concrete Sample Thickness (cm)	LAC $\mu_L$ ( $\text{cm}^{-1}$ )	LAC Average $\mu_L$ ( $\text{cm}^{-1}$ )
0.0	04	0.3975	0.24380
	08	0.2453	
	12	0.1860	
	16	0.1464	
0.5	04	0.3873	0.24240
	08	0.2499	
	12	0.1860	
	16	0.1464	
1.0	04	0.3975	0.24380
	08	0.2453	
	12	0.1860	
	16	0.1464	
3.0	04	0.3960	0.24430
	08	0.2493	
	12	0.1829	
	16	0.1490	

Table 6.6 MAC Average Calculation

WSIO %	Concrete Sample Thickness (cm)	MAC $\mu_M$ ( $\text{cm}^{-1}$ )	MAC Average $\mu_M$ ( $\text{cm}^{-1}$ )
0.0	04	0.1506	0.09160
	08	0.0929	
	12	0.0688	
	16	0.0541	
0.5	04	0.1474	0.09230
	08	0.0951	
	12	0.0722	
	16	0.0544	

1.0	04	0.1526	0.09380
	08	0.0946	
	12	0.0721	
	16	0.0599	
3.0	04	0.1523	0.09368
	08	0.0963	
	12	0.0690	
	16	0.0571	

**6.1.3. Apparent and Calculated Densities**

(Table 6.7 and 6.8) shows the average of apparent density (AD) and calculated density (CD) for the various WSIO (0.0%, 0.5%, 1.0%, and 3.0%) at different concrete samples thickness (4cm, 8cm, 12cm, and 16 cm). Figure 6.9 and 6.10, showing the those relations. Based on the Figure (6.9), it's observed that the average AD increases as the WSIO % was increased, the maximum % increases in AD was 1.45 % at WSIO 30 %, and based on the Figure

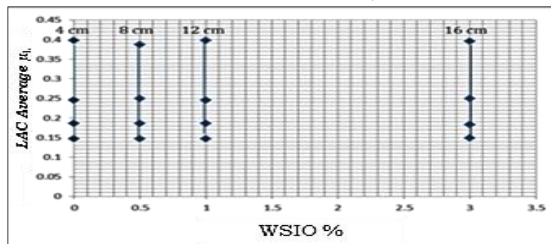


Figure 6.7 LAC Average Vs. WSIO %

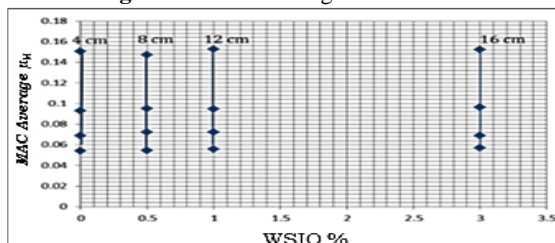


Figure 6.8 MAC Average Vs. WSIO %

**Table 6.7 Average of Apparent Density (AD)**

Concrete Sample Thickness (cm)	WSIO %	AD $\rho(g\text{ cm}^{-3})$	AD Average $\rho(g\text{ cm}^{-3})$
04	0.0	2.6392	2.61765
	0.5	2.6276	
	1.0	2.6042	
	3.0	2.5996	
08	0.0	2.6527	2.62565
	0.5	2.6409	
	1.0	2.6057	
	3.0	2.6033	
12	0.0	2.7161	2.64055
	0.5	2.5908	
	1.0	2.5932	
	3.0	2.6621	
16	0.0	2.7036	2.65553
	0.5	2.6872	
	1.0	2.6189	
	3.0	2.6124	

**Table 6.8 Average of Calculated Density (CD)**

Sample Thickness (cm)	WSIO %	CD $\rho_s(g\text{ cm}^{-3})$	CD Average $\rho_s(g\text{ cm}^{-3})$
04	0.0	2.5433	2.58860
	0.5	2.5383	
	1.0	2.6726	
	3.0	2.6002	
08	0.0	2.5947	2.60120
	0.5	2.6413	
	1.0	2.5792	
	3.0	2.5894	

12	0.0	2.6952	2.62550
	0.5	2.5793	
	1.0	2.5758	
	3.0	2.6516	
16	0.0	2.9066	2.70520
	0.5	2.6187	
	1.0	2.6861	
	3.0	2.6095	

(6.10), it's observed that the average CD increases as the thickness of concrete sample was decreased, the maximum % increasing in CD was 4.31 % at WSIO 30 %.

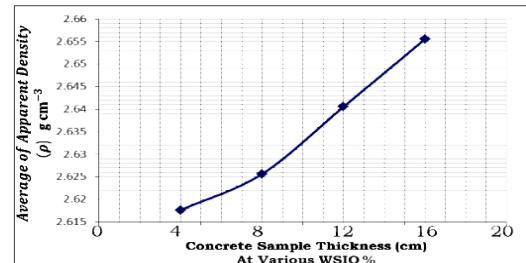


Figure 6.9 Average of AD vs. Samples Thickness at Different WSIO %

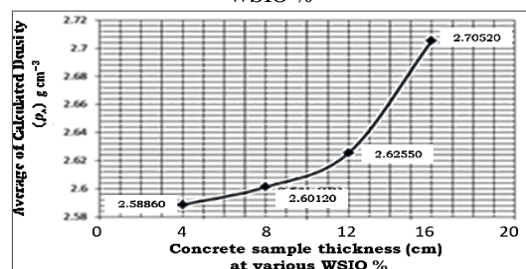


Figure 6.10 Average of CD vs. Samples Thickness at Different WSIO %

**7. Effects of WSIO % on the Compression Strength of the Concrete Samples**

The samples were compressed using ELE international machine Model with load speed of 100 N/s, as shown in (Figure 7.1). The experimental results were obtained in (kN) values. According to the produced data, the value of the failure stresses (MPa) for each sample is extracted. The (%) percentages of increase in the failure stresses are also calculated.



Figure 7.1 Concrete Sample under Failure of Compression Load

The cylindrical samples with dimensions of (7.62cm) diameter and lengths (4 cm), (8 cm), (12 cm), and (16 cm) were prepared for testing a compressive strength. The concrete mixes with varying WSIO (0% , 0.5%, 1.0%, and 3.0%) iron weight as partial replacement of sand were casted into cylindrical plastic molds for subsequent testing. Each sample was divided into three sub-specimens. Before the test was carried out, each sample was grinded and polished in order to obtain a balanced surface to get accurate results. The number of prepared concrete sample in the present research were 48 as shown on Figure (7.2) The load was applied axially without shock till sample was crushed. The results are presented in (Table 7.1). The relation between compressive strength and WSIO % is showed on (Figure 7.3). It can be observed that the addition of iron oxide to the Portland cement depends highly on both the WSIO % and the thickness of the concrete sample. When the thickness of the concrete sample was 4 cm, the compressive strength was improved at WSIO 0.5% but it was declined as WSIO increased

to 1.0% and more further to 3.0%. Again at concrete sample thickness 8 cm, the compressive strength was improved at WSIO 0.5% and declined as same as in the case of 4 cm concrete sample. The improvement of compressive strength in the cases of 12 cm and 16 cm concrete samples was not clearly identified. In general, the addition of WSIO to

the concrete may improve the compressive strength, but still depends on the concentration of iron oxide as well as the thickness of the concrete. The un-stability of compressive strength with addition of WSIO may attributed to the formation of porosity of iron oxide as shown on (Figure 7.4). The more WSIO addition, the more pores were appeared inside of iron oxide regions [14].



Figure 7.2. Concrete Samples Prepared for the Compression

Table 7.1. The Compression Strength Results

Concrete Sample Thickness (cm)	Sample No.	WSIO %	Average Load $\times 10^3$ (N)	Compressive Strength (kPa)
04	M1	0.0	11.30	118
	N1	0.5	24.00	125
	P1	1.0	33.30	116
	R1	3.0	42.00	110
08	M2	0.0	04.67	049
	N2	0.5	22.67	118
	P2	1.0	26.00	090
	R2	3.0	37.67	098
12	M3	0.0	04.00	042
	N3	0.5	11.83	062
	P3	1.0	22.00	077
	R3	3.0	22.00	057
16	M4	0.0	04.00	042
	N4	0.5	08.33	043
	P4	1.0	21.67	075
	R4	3.0	30.67	080

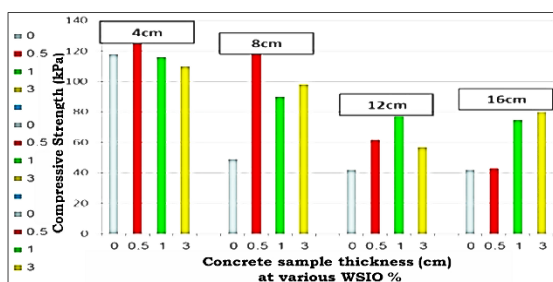


Figure 7.3. Compressive Strength vs. WSIO %

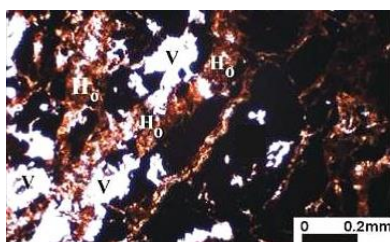


Figure 7.4 Iron Oxide Aggregates have high porosity, voids (V)

which have appeared during formation of iron oxide  $H_o$  [14]

## 8. Conclusions

Wadi Al-Shatti Iron Oxide (WSIO) was used in various weights % to investigate its ability to be used as a shielding material as well as studying their effects on the compressive strength of the hardened concrete. The Linear Attenuation Coefficients (LAC), Mass Attenuation Coefficients (MAC), Apparent Density (AD) and Calculated Density (CD) showed that the ore material used in the present study may be preferred as shielding material against  $\gamma$  -ray radiation. It is clear from the results that as the sample thickness increases, the detector intensity decreases as well and when WSIO % increases, the LAC increases as well. On the other hand, the MAC decreases thus, this indicated that the main absorption operations such as photo effect, Compton effect were occurred depending on the photon energy from the source (Cobalt 60). The CD increases as the concrete sample thickness increases and also as the WSIO % increases, this indicating that, the CD has a physical property. The results also showed that the addition of WSIO % can enhanced the compression strength of hardened concrete specially in those samples with WSIO lower than 3.0 % and those with thick sizes.

In general, the addition of low contents of WSIO % to the concrete slightly improving the radiation attenuation of concrete and may improving the compressive strength, but still depends on the of WSIO % as well as the size of the concrete.

## 9. References

- [1]- Mehta, P. K., and Monteiro, P. J. M., NJ, (1993) *Concrete, structure, properties and materials, 2nd Ed.*, Prentice Hall, Upper Saddle River.
- [2]- Fahlman, BD., (2007). *Materials Chemistry*. Springer. Pp. 282 .
- [3]- Akkurt, I., Başıyigit, C., Akkaş, A., Kılınçarslan, Ş., Mavi, B., and Günoğlu, K., (2012), "Determination of some heavyweight aggregate half value layer thickness used for radiation shielding" *Acta Phys. Pol. A*, 121(1 , 138) – 140 .
- [4]- R. Lambert J. H., (2001), *Photometry, or. The measure and gradations of light, colors and shade*, SBN: 0879951796, Germany.
- [5]- Dukhin, A.S. and Goetz, P.J., (2002), "Ultrasound for characterizing colloids", Elsevier.
- [6]- H. Eschrig, (2003), *The Fundamentals of Density Functional Theory*, Institute for Solid State and Materials Research Dresden, Dresden, Germany.
- [7]- FathiHabashi, (1997), *Hand Book of Extractive Metallurgy, Volume I, The Metal Industry, Ferrous Metals*, Lava University, Department of Mines and Metallurgy, Canada.
- [8]- Buzea, C., Pacheco, I., Robbie, K., (2007), "Nanomaterials and Nanoparticles: Sources and Toxicity". *Biointerphases* Vol. 2, pp. MR17 .
- [9]- Mostofinejad, D, Rezaei, M, and Shirani, A., (2012), "Mix design effective parameters on gamma ray attenuation coefficient and strength of normal and heavyweight concrete" *Constr. Build. Mater.*, 28(1), 224–229 .
- [10]- Ouda, A. S., (2015), "Development of high - performance heavy density concrete using different aggregates for gamma-ray shielding" *Prog. Nucl. Energy*, 79, 48–55 .
- [11]- Indian Standard, (1998), *Portland Slag Cement-Specification IS455: 1888*, (Reaffiud 1995), Forth Revision.
- [12]- Altasakheer, *Pure Mineral Water*, (2019), Hajarah, Sebha City, near musical Institute, Tele:0925137161.
- [13]- Ali M. Tajourit, et. al., (2013), *Qemscan Analysis Of Wadi Al-Sitatti Iron Ore (Libya)*, Materials & Metallurgical Eng., Faculty of engineering, U T, Libya, TMS (TheMinqats, Metals & Materials Society).
- [14]- Osman Gencil, et. al., (2010), *Concretes Containing Hematite for Use as Shielding Barriers*, Department of Civil Engineering, Faculty of Engineering, Bartın University, 74100 Bartın, Turkey, ISSN 1392 – 1320 MATERIALS SCIENCE (MEDZIAGOTYRA). Vol. 16, No. 3 .